EUROPEAN ORGANIZATION FOR NUCLEAR RESEARCH

February 1988

STATES OF HIGH ENERGY DENSITY

MICHAEL MURRAY

HELIOS Collaboration
UNIVERSITY OF PITTSBURGH
PITTSBURGH, PA

ABSTRACT

The transverse energy, E_T, spectra for O^{16} and S^{32} incident for various elements at 200 GeV/nucleon are shown. The target and projectile dependencies of the data are discussed. The energy density achieved is estimated. For O^{16} on Tungsten the multiplicity spectrum is also presented as well as the pseudorapidity spectra as a function of the transverse energy. The multiplicity cross section $d\sigma/dN$ as measured in the backward hemisphere ($0.9 < \eta < 2.9$) is found to be very similar in shape to the transverse energy distribution $d\sigma/dE_T$ reflecting the particular geometry of nucleus nucleus collisions. The dependence on the atomic mass of the target, A_T and projectile A_P is not what one would expect from naive considerations.

DISCLAIMER

1. INTRODUCTION

Presently several experiments at CERN and BNL are searching for the Quark Gluon Plasma, **QGP**, through collisions of heavy ions with nuclear targets. A prerequisite of this search is that states of sufficiently high energy density be found. Such states should produce very high multiplicity and transverse energy, E_T. Thus the spectra of E_T and multiplicity are of great interest since they show whether it is possible to produce the QGP. Here the E_T and multiplicity spectra for oxygen and sulphur on various targets will be discussed. The shape of these spectra is well described by a simple geometrical model.

2. SETUP

The parts of **HELIOS** used in this analysis are shown in Figure 1. HELIOS has optimised its calorimetry to find the highest possible E_T in the target fragmentation region. By triggering on E_T in the pseudorapidity, η, region -0.1 to 2.9, we look for spherical fireballs at rest in the centre of mass frame. The E_T in the forward calorimeter was measured but was not part of the trigger.

We define the transverse energy:

$$E_T = \Sigma_i E_i \sin\theta_i$$

where E_i is the kinetic energy for baryons and the total energy for all other particles. Also the pseudorapidity, $\eta = -ln\tan\frac{\theta}{2}$.

The HELIOS calorimetry is of the sampling type with plastic scintillator as the active medium and uranium or uranium and copper absorber plates. Each module is 120 cm x 20 cm in cross sectional area and about four interaction lengths thick. Each stack is divided into 6 towers. The calorimetry is described in detail in references [1,2] the E_T analysis in [3]. Charged particles are measured in a set of two silicon detectors positioned 3 and 9 cm, respectively, downstream from the thin W target. Both are 300 μm thick, fully depleted, and equipped with pad readout for multiplicity and two dimensional position information.

The first silicon ring counter, covering $0.9 < \eta < 2.9$, is divided into 384 segments, forming 12 sectors and 32 rings approximately equally spaced in pseudorapidity see Figure 1. The second silicon detector [8]. covering $2.9 < \eta < 5.0$, consists of an array of 400 silicon pad segments varying in size rom 0.02 × 0.167 to 0.167 × 0.66 cm^2. The multiplicity analysis is described by Schukraft [9].

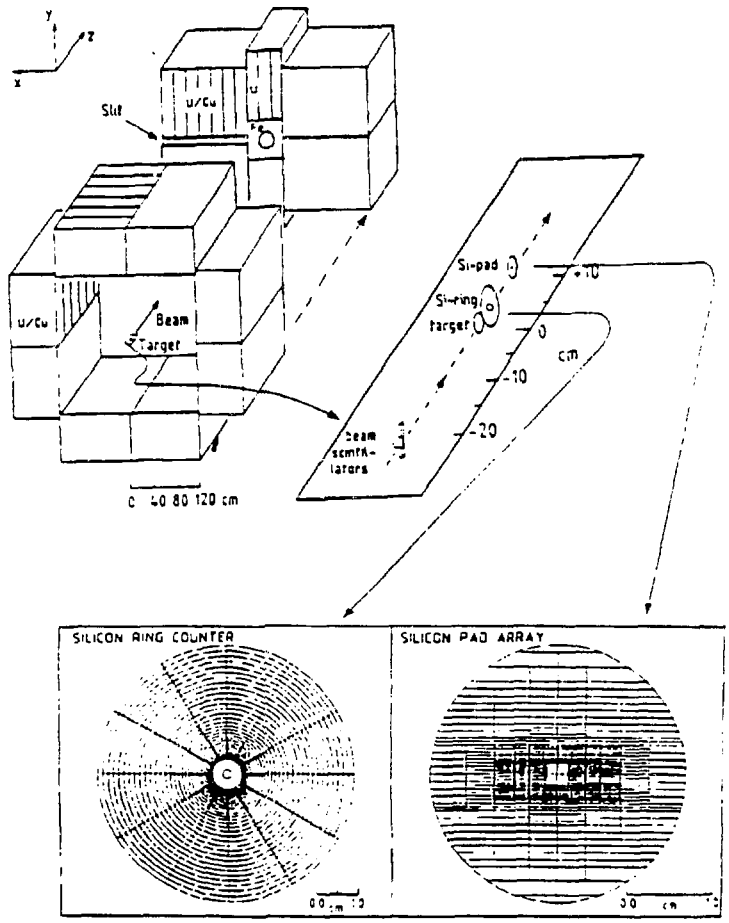

Figure 1: The calorimeters used in the analysis with the silicon counters. The target is surrounded by a box consisting of a calorimetrised dipole magnet, U/scintillator and U/Cu/scintillator modules.

3. RESULTS

3.1 Transverse Energy Spectra

The E_T spectra for oxygen on various targets at 60 and 200 GeV/nucleon are shown in Figure 2. The general shape of the spectra is made up of a fall , followed by a plateau and a steeply falling tail. This shape can be explained by a simple geometrical model, see [6,7,4]. Here the collision is represented as the sum of separate nucleon nucleon collisions. The total number of collisions is determined by the overlap integral of the possibly nonspherical, colliding nuclei. This E_T generated in each nucleon nucleon collision has a gaussian distribution. The mean and variance of this distribution are fitted to our spectra and give excellent fits, see Figure 2. In Figure 2 it is interesting to note that the observed maximum E_T corresponds to 70% of the kinematic limit. This implies an energy density of 3 to 5 GeV/fm^3 depending on the number of target nucleons involved in the collision.

The E_T spectra for sulphur on various targets at 200 GeV/ nucleon are shown in Figure 3. The spectrum of S^{32} on Al^{27} ,Figure 3, is unusual in that it has no plateau. This is simply because the $S^{32}$and Al^{27} nuclei are approximately symmetric. The crossing of the Pt and W curves is due to the greater deformation of W relative to Pt. For peripheral and low E_T collisions this is a second order effect but it becomes more important at high E_T. This is because it is easier to produce high E_T by increasing the violence of a fixed number of collisions. Thodberg, [5] has shown that for high E_T collisions W is completely aligned along the beam axis.

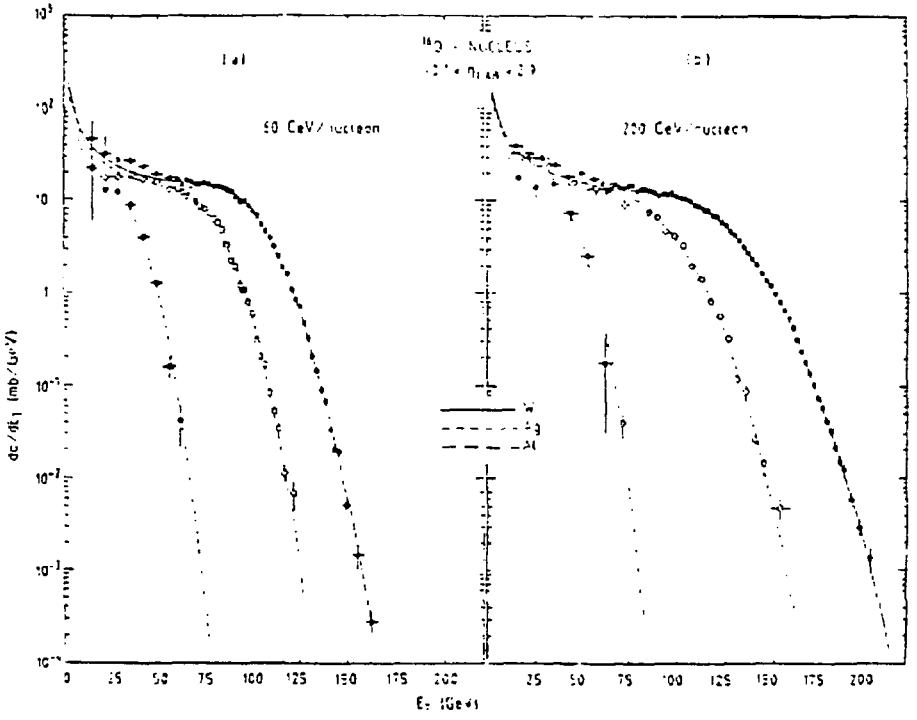

Figure 2: Geometrical parametisation fits to $d\sigma/dE_T$ at 60 and 200 GeV per nucleon. O^{16} W (closed circles), O^{16} Ag (open squares) and O^{16} Al (closed squares).

3.2 Multiplicity Spectra

The multiplicity spectra for O^{16} incident on Al, Ag, and W targets at 200 GeV/nucleon are shown in Figure 4 for the 2 different η coverages of our silicon counters. These have the same features as the E_T spectra. The corresponding pseudorapidity distributions $dN/d\eta$ are shown in Figure 5. Spectra are drawn for events from the plateau, central and tail regions of the E_T spectrum. Note that the peak moves backward with increasing E_T. Somewhat surprisingly the forward regions do not seem to get depleted with increasing E_T. For high, E_T, dN/dη becomes bell shaped, corresponding to a spherical fireball radiating uniformly in the centre of mass.

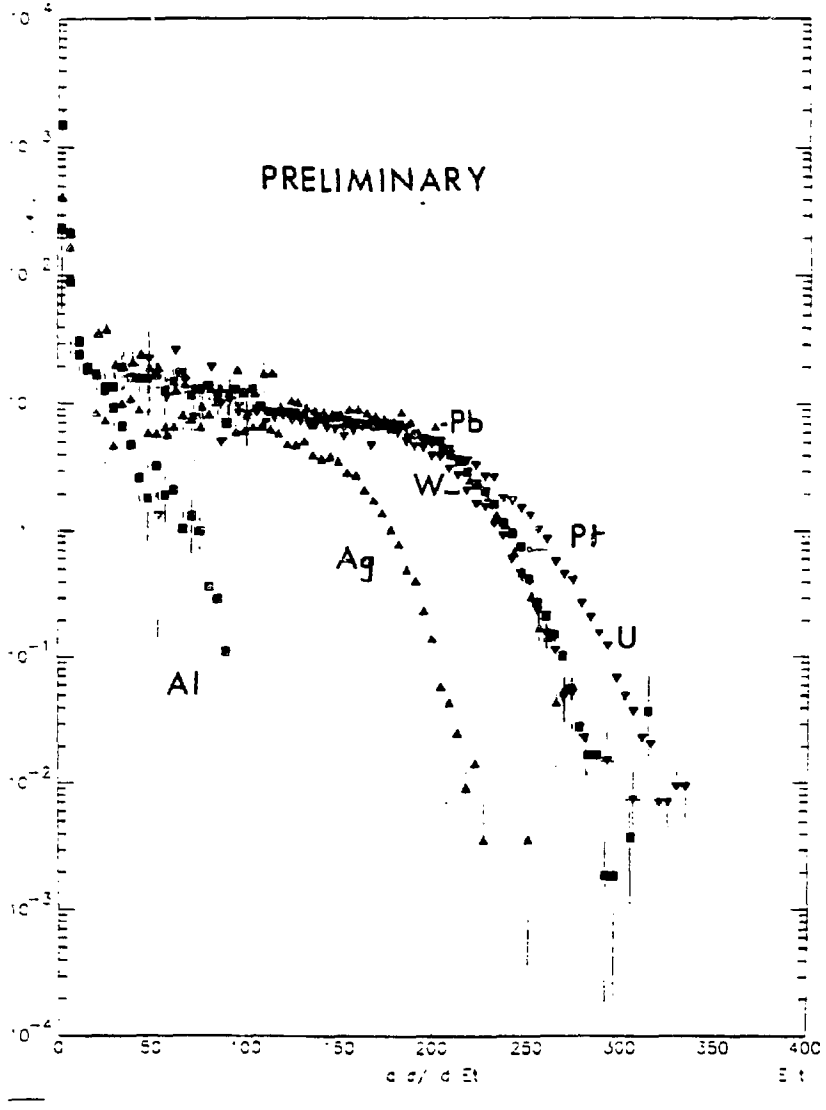

Figure 3: The Et spectra dN/d E_T for S on various targets. The spectra are preliminary and have yet to be deconvoluted for calorimeter resolution.

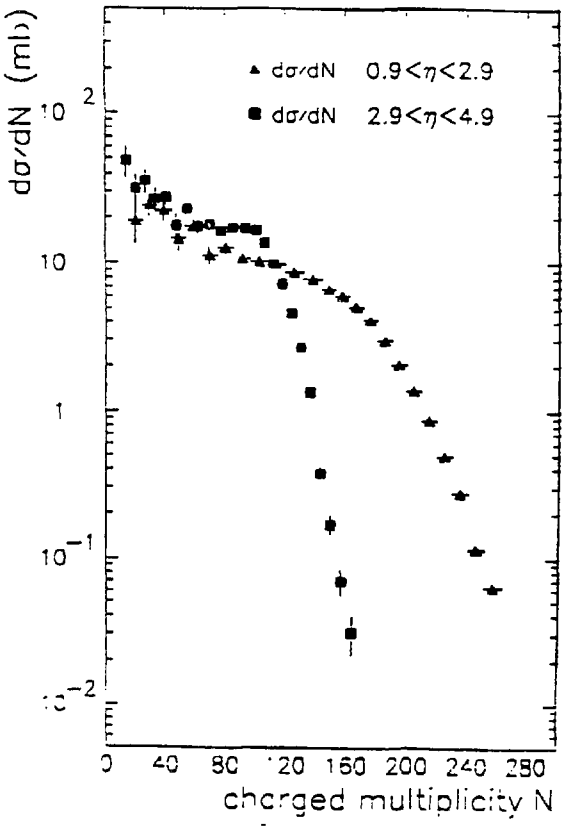

Figure 4: Multiplicity spectra, $d\sigma/dN$ for O^{16} on W at 200 GeV/nucleon. $0.9 < \eta < 2.9$ (open circles) and $2.9 < \eta < 4.9$ (closed circles). The error bars shown are statistical only, the global systematic error on the multiplicity scale is 8%.

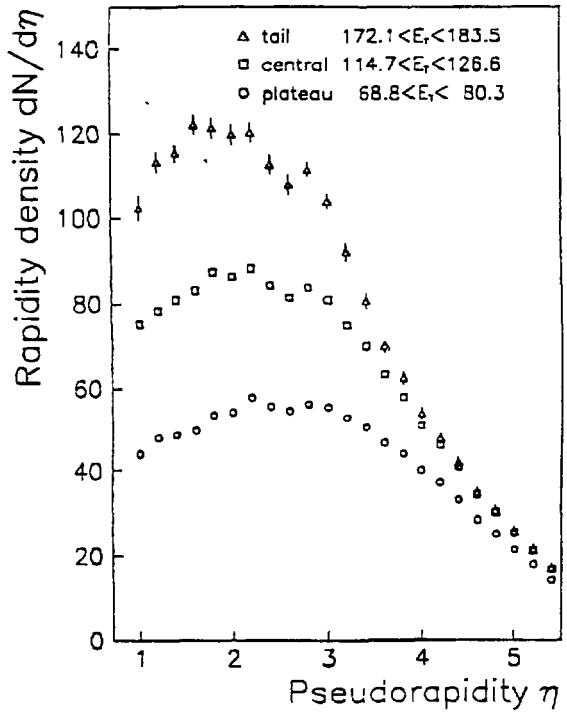

Figure 5: Distribution of multiplicity in η for 3 windows of E_T. The errors shown are statistical only.

4. CENTRAL COLLISIONS

To compare the E_T generated by collisions of different nuclei, it is convenient to define the concept of **central collisions**. We would like this to mean collisions with impact parameter **b** = 0. Since such a collision has zero cross section, σ , and b is not directly measurable we make the following operational definitions:

$E_T^{CENTRAL} = E_T$ for which $\sigma = .5\sigma_{CENTRAL}$

$\sigma_{CENTRAL} = \sigma$ for which $\frac{d\sigma}{dE}$ is a minimum.

4.1 Target dependence

The dependence of $E_T^{CENTRAL}$ on A_p and A_T for O^{16} and $S^{32}$is shown in Figure 6. Note that $E_T^{CENTRAL}$ increases with energy. For $A_T = O^{16}, E_T^{CENTRAL} \propto A^{.5}$ but for sulphur this is $E_T^{CENTRAL} \propto A^{.33 \pm .1}$. The rise in $E_T^{CENTRAL}$ with A_T indicates that we are above the full stopping regime.

4.2 Projectile Dependence

The rise in the $E_T^{CENTRAL}$ from O^{16} to S^{32} is slower than one would expect from simple geometry. From O^{16} to S^{32}, one would expect $E_T^{CENTRAL}$ to increase from geometry by a factor of 1.9. However, $E_T^{CENTRAL}$ rises as $A_p^{\frac{2}{3}}$ implying that the energy density does not increase with A_p.

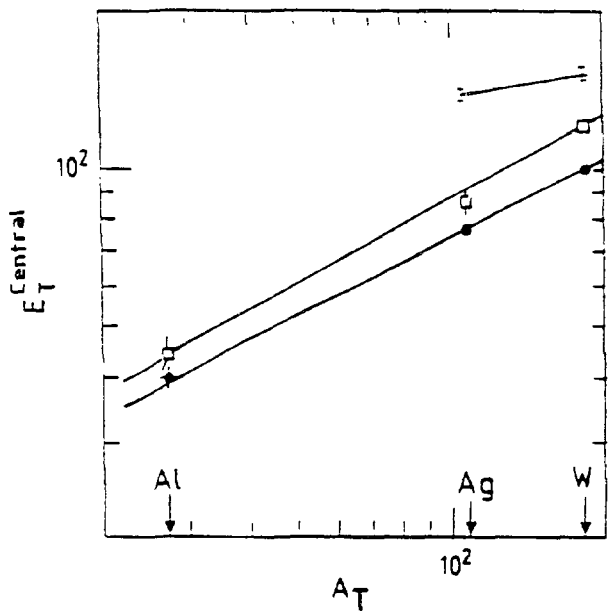

Figure 6: $E_T^{central}$ versus A_T for O^{16} at 60 (lower) and 200 GeV/nucleon (middle). The upper line is for S^{32} at 200 GeV/nucleon. The solid lines represent fits to the data of the form A^{α} where α = 0.48±.02, 0.53±.04 and 0.30±07 for O^{16} at 60 and 200 and S^{32} at 200 GeV/nucleon respectively.

5. CONCLUSIONS

The gross features of E_T and multiplicity spectra can be explained by a simple geometrical approach. Energy densities of 3 to 5 GeV/fm^3 seem achievable. This figure seems independent of the projectile. As E_T increases the multiplicity distribution moves backward. Its shape is consistent with a spherical fireball at rest in the centre of mass frame.

This work has been supported in part by the U.S. Dept. of Energy under contract DE-AC02-76CH00016.

References

1. Åkesson et al., *Nucl. Instrum. Methods* **A241** (1985) 17.

2. Åkesson et al., *preprint CERN – EP/87 – 111 to be published in Nucl. Instrum. Methods.*

3. Åkesson et al., *preprint CERN – EP/87 – 176 to be published in Zeitschrift für Physik C.*

4. Thodberg, H. H. , *Internal HELIOS note 219 (1987).*

5. Thodberg, H. H. , *Internal HELIOS note 237 (1987).*

6. Baym G., Braun – Munzinger P. and Ruuskanen V., *Phys Lett.* **B190** (1987) 29.

7. Jackson A. D., and Bøggild H., *Nucl. Phys.* **A470** (1987) 669.

8. Beuttenmuller et al., *Nucl. Instrum. Methods* **A252** (1986) 471.

9. Schukraft J., *Proceedings of QM87 ,to be published in Zeitshrift für Physik C.*